HHS Public Access

Author manuscript

Prostate. Author manuscript; available in PMC 2024 December 05.

Published in final edited form as:

Prostate. 2023 November ; 83(15): 1458–1469. doi:10.1002/pros.24602.

Downregulation of EZH2 inhibits epithelial–mesenchymal transition in enzalutamide-resistant prostate cancer

Zhuangzhuang Zhang, PhD[1,2], **Xinyi Wang, MSc**[1,2], **Miyeong Kim, PhD**[1,2], **Daheng He, PhD**[2], **Chi Wang, PhD**[2], **Ka Wing Fong, PhD**[1,2], **Xiaoqi Liu, PhD**[1,2]

[1]Department of Toxicology and Cancer Biology, University of Kentucky, Lexington, Kentucky, USA

[2]Markey Cancer Center, University of Kentucky, Lexington, Kentucky, USA

Abstract

Background: Androgen signaling inhibitors (ASI) have been approved for treatment of metastatic castration-resistant prostate cancer (mCRPC). However, the limited success of ASI in clinic justifies an urgent need to identify new targets and develop novel approaches for treatment. EZH2 significantly increases in prostate cancer (PCa). Little is understood, however, regarding the roles of EZH2 in Enzalutamide-resistant (EnzR) mCRPC.

Methods: We firstly investigated the levels of EZH2 and the altered pathways in public database which was comprised with primary and metastatic PCa patient tumors. To elucidate the roles of EZH2 in mCRPC, we manipulated EZH2 in EnzR PCa cell lines to examine epithelial-mesenchymal transition (EMT). To dissect the underlying mechanisms, we measured the transcription levels of EMT-associated transcription factors (TFs).

Results: We found that EZH2 was highly expressed in mCRPC than that of primary PCa tumors and that EnzR PCa cells gained more EMT characteristics than those of enzalutamide-sensitive counterparts. Further, loss of EZH2-induced inhibition of EMT is independent of polycomb repressive complex 2 (PRC2). Mechanistically, downregulation of EZH2 inhibits transcription of EMT-associated TFs by repressing formation of H3K4me3 to the promotor regions of the TFs.

Conclusion: We identified the novel roles of EZH2 in EnzR mCRPC. EnzR PCa gains more EMT properties than that of enzalutamide-sensitive PCa. Loss of EZH2-assocaited inhibition of EMT is PRC2 independent. Downregulation of EZH2 suppresses EMT by impairing formation of H3K4me3 at the promotor regions, thus repressing expression of EMT-associated TFs.

Correspondence: Xiaoqi Liu, PhD, Department of Toxicology and Cancer Biology, University of Kentucky, 1095 V.A. Dr, Lexington, KY 40536, USA. xiaoqi.liu@uky.edu; Fax: 859-323-1059.

AUTHOR CONTRIBUTIONS

Zhuangzhuang Zhang and Xinyi Wang conceived the project, designed/performed experiments, and interpreted data. Zhuangzhuang Zhang and Xiaoqi Liu over-saw the project and co-wrote the manuscript. Miyeong Kim and Ka Wing Fong contributed to ChIP-PCR analysis. Daheng He and Chi Wang contributed to bioinformatic data analysis.

Disclosure of Potential Conflicts of Interest: The authors declare no potential conflicts of interest.

CONFLICTS OF INTEREST STATEMENT

The authors declare no conflicts of interest.

SUPPORTING INFORMATION

Additional supporting information can be found online in the Supporting Information section at the end of this article.

Keywords

EMT; enzalutamide-resistance; EZH2; H3K4me3; prostate cancer

1 | INTRODUCTION

Since androgen receptor (AR) signaling continues to be essential for prostate cancer (PCa) progression even after castration, targeting AR signaling should be an effective approach for the treatment of patients with castration-resistant prostate cancer (CRPC). Metastatic disease is present in >80% of patients with CRPC. Until recently, treatment options for metastatic CRPC (mCRPC) have been chemotherapy with docetaxel with limited success. Androgen signaling inhibitors (ASI), such as enzalutamide and abiraterone acetate, have been approved to treat mCRPC.[1,2] However, the limited efficacy of ASIs justifies an urgent need to identify new targets and develop novel approaches to treat ASI-resistant CRPC.

Discovery of EZH2 (enhancer of zeste homolog 2), the catalytic subunit of the Polycomb Repressive Complex 2 (PRC2) responsible for H3K27 trimethylation, as a robust biomarker for PCa sheds new light on developing potential therapeutic approaches.[3] In addition to the canonical function of EZH2 as a histone methyltransferase, accumulated evidence showed that EZH2 can also mediate methylation of non-histone proteins substrates, mostly through PRC2-dependent but sometimes PRC2-independent mechanisms, with varying consequences. For example, EZH2 methylation of JARID2 and Elongin A regulates global transcription.[4,5] In addition to general transcriptional regulation, EZH2 also controls several specific transcription factors. For example, EZH2-associated methylation of STAT3 leads to STAT3 activation and increased transcription of STAT3-targeted genes.[6] EZH2-mediated methylation of GATA4 reduces its interaction with and acetylation by p300, thereby inhibiting GATA4 transcriptional activity.[7] Besides regulating the transcriptional activities of substrates, EZH2-mediated methylation has also been shown to play a critical role in substrate ubiquitination and protein degradation. For example, EZH2 methylation of orphan nuclear receptor RORα promotes its ubiquitin-dependent degradation,[8] while methylation of FOXA1 removes FOXA1 ubiquitination and enhances its protein stability.[9] EZH2 functions can be dynamically altered by posttranslational modifications, including ubiquitination, acetylation, o-GlcNAclation, and sumoylation.[10] In addition, EZH2 phosphorylation and methylation also regulate EZH2 functions. It was initially discovered in breast cancer that AKT1 phosphorylates EZH2 at S21 to reduce its affinity for canonical substrate histone H3.[11] Besides AKT1, mitogen-activated protein kinase 14 (MAPK14), has been shown to phosphorylate EZH2 at threonine 372 (T372), leading to the formation of repressive chromatin on the Pax7 promoter.[12] PRC2 auto-methylates EZH2 and SUZ12 in the presence or absence of nucleosomal substrates.[13]

EZH2 is highly upregulated in aggressive PCa and plays an important role in promoting PCa progression. EZH2 downregulation has been shown to induce G2/M cell cycle arrest, abolish cell proliferation and invasion in vitro, and quench tumor growth in vivo, while EZH2 overexpression has been shown to promote oncogenic behaviors.[14–18] Much of these activities have been associated with EZH2-mediated epigenetic silencing of

tumor suppressor genes.[19] EZH2 has also been shown to exhibit a polycomb-independent oncogenic function to act as a coactivator of AR in CRPC cells.[20] Recently, Yuan et al.[21] reported that SETD2 methylation of EZH2 promotes EZH2 degradation, thus delaying PCa metastasis. Bai et al.[22] reported that inhibition of EZH2 could overcome enzalutamide resistance by impairing its binding to the promotor of prostate-specific antigen (PSA). However, the potential role of EZH2 in the metastasis of CRPC, particularly in enzalutamide-resistant (EnzR) CRPC is still poorly understood.[21]

In this study, we found that more EMT properties were gained in EnzR cells than that in enzalutamide-sensitive cells. By exploring the data sets, we identified EZH2 as a potential driver for mCRPC. Downregulation of EZH2 inhibited EMT in EnzR PCa cells via suppressing the expression of EMT-associated transcription factors (TFs). Mechanistically, downregulation of EZH2 impairs the formation of H3K4me3 histone mark at the promotors of EMT-associated TFs, consequently resulting in the inhibition of EMT. These data suggest the distinct role of EZH2 in the metastasis of EnzR CRPC beyond its well-known PRC2-dependent role in cancer.

2 | MATERIALS AND METHODS

2.1 | Public data sets

(1) The Taylor et al.[23] data set, which has 29 normal, 131 primary tumor, and 19 metastatic tumor samples, and (2) The Grasso et al.[24] data set, which contains 28 benign, 59 localized cancer, and 34 metastatic CRPC samples.

2.2 | Cell lines

The following cell lines have been used: LNCaP, MR49F, C4-2, C4-2R, $ARCaP_E$, and $ARCaP_M$. Among them, LNCaP is androgen dependent, whereas C4-2 is derived from LNCaP but androgen independent. MR49F and C4-2R cells, derived from LNCaP and C4-2, respectively, are both enzalutamide-resistant. All cell lines were tested and found to be free of mycoplasma according to the manufacturer's recommendations. All cell types were checked for proper morphology before every experiment and consistently monitored for changes in cell replication that might suggest mycoplasma contamination. Short Tandem Repeat (STR) profiling, provided by ATCC, was used for testing and authentication of all cell lines. All cells were within 50 passages and Mycoplasma was detected every 3 months using MycoAlert PLUS Mycoplasma Detection Kit (Lonza, LT07-705).

2.3 | Reagents

Antibodies against EZH2, E-cadherin, N-cadherin, Twist, Vimentin, Snail, GAPDH, β-actin, H3K27me3, H3K4me3, Histone H3, Myosin IIB, β-catenin, and CK19 were purchased from Cell Signaling Technology (CST). While hJAM-A antibody was purchased from R&D systems, lentivirus particles against EZH2 were purchased from Sigma.

2.4 | Public gene expression data sets and clinical datasets analysis

For the Grasso and Taylor microarray data sets, we used the "limma" R package to perform differential analysis and identified significantly differentially expressed genes with a false

discovery rate (FDR) of less than 0.05. Then we calculated the rank of each gene based on its signed log p-value from the differential analysis results. We then used the "ggplot2" R package to generate a 2-D density plot. We selected the DE genes that were commonly expressed in both Grasso and Taylor data sets and had consistent signs of log2-fold change. We used the "clusterProfiler" R package with default settings (based on Fisher's exact test algorithm) to perform gene ontology (GO) and Kyoto Encyclopedia of Genes and Genomes (KEGG) pathway enrichment analysis. Heatmaps for the genes of pathways of interests based on both Grasso and Taylor data were generated by using the R package "pheatmap". To allow for the horizontal visual comparison between the Grasso and Taylor data, the order of genes shown on the heatmaps were manually specified and no automatic clustering was applied.

2.5 | Immunofluorescence (IF) staining

Cells were incubated with indicated antibodies for 1 h at room temperature, followed by incubation with secondary antibody and 4' 6-diamidino-2-phenylindole (DAPI; Sigma) for 1 h at room temperature avoiding light.

2.6 | Immunoblotting (IB)

Cell lysates were prepared in TBSN buffer (20mM Tris, pH 8.0, 150mM NaCl, 0.5% Nonidet P-40, 5mM EGTA, 1.5mM EDTA, and 20mM p-nitrophenyl phosphate). For IB, membranes were incubated with specific antibodies at 4°C for overnight, followed by additional incubation with the secondary antibody for 1 h at room temperature.

2.7 | Real-time quantitative polymerase chain reaction (RT-qPCR) analysis

Total RNA was isolated using TRIzol (Thermo Fisher Scientific) and reversely transcribed into cDNA using SuperScript III First-Strand Synthesis System (Life Technologies) according to the manufacturer's instructions. Real-time PCR was performed using an ABI 7900HT thermal cycler and the FastStart Universal SYBR Green Master (Roche, Basel, Switzerland). The data were normalized to the amount of GAPDH transcript. The primer sequences were as follows: N-cadherin: 5′-TGGGAATCCGACGAATGG-3′ (forward) and 5′-GCAGATCGGACCGGATACTG-3′ (reverse); Fibronectin: 5′-CATGAGACTGGTGGTTACATGTTAGA-3′ (forward) and 5′-GCATGATCAAAACACTTCTCAGCTA-3′ (reverse); SNAIL: 5′-ACCCCAATCGGAAGCCTAAC-3′ (forward) and 5′-GCTGGAAGGTAAACTCTGGATTAGA-3′ (reverse); SLUG: 5′-CAGCTACCCAATGGCCTCTCT-3′ (forward) and 5′-GGACTCACTCGCCCCAAAG-3′ (reverse); ZEB1: 5′-CAAATGTGGAAAGCGCTTCTC-3′ (forward) and 5′-GTAGGAGTAGCGATGATTCATGTGTT-3′ (reverse); ZEB2: 5′-CGCATTTCCCCCTGCTACT-3′ (forward) and 5′-TGGTCGTAGCCCAGGAATACTG-3′ (reverse); TWIST: 5′-GGAGTCCGCAGTCTTACGAG-3′ (forward) and 5′-TCTGGAGGACCTGGTAGAGG-3′ (reverse); GAPDH: 5′-GAAATCCCATCACCATCTTCCA-3′ (forward) and 5′-CCAGCATCGCCCCACTT-3′ (reverse).

2.8 | Invasion and migration assay

After cells were infected with lentivirus-depleting EZH2 for 48 h, 3μg/mL puromycin was administrated to select for another 72 h. Selected cells (4×10^4) were seeded into the upper chamber of a 24-well transwell chamber (#3422). An aliquot of 500 μL culture medium supplemented with 10% fetal bovine serum (FBS) was added into the lower part of the chamber. Cell culture medium with 0.5% FBS replaced the medium in the lower well of the chamber. After incubation for different time, cells in the upper well were removed with a cotton swab. Cells that migrated into the opposite side of the upper well were washed with phosphate-buffered saline (PBS), fixed in 4% paraformaldehyde, and stained with coomassie blue dye. For transwell invasion assay, the cells of the upper well of the transwell were coated with 50 μL (1 μg/mL) Matrigel (#356234; BD). The Matrigel was allowed to harden at 37°C in a 5% CO_2 incubator for 4 h and then cells (4×10^4) were seeded into the upper chamber of a 24-well transwell chamber.

2.9 | Chromatin immunoprecipitation (ChIP)

Cultured cells were cross-linked with 1% formaldehyde for 10 min and the cross-linking was quenched by 0.125M glycine for 5 min at room temperature. After cells were then rinsed with cold 1×PBS twice, the following steps were performed at 4°C. Cell pellets were lysed by cell lysis buffer (5mM PIPES, pH 8.0, 85mM KCl, 0.5% NP40) with protease inhibitor (Roche) for 10 min. Nuclei pellets were spun down at 5000 rpm for 5 min, resuspended in nuclear lysis buffer (50mM Tris-Cl, pH 8.0, 10mM EDTA, and 1% sodium dodecyl sulfate [SDS]), and then incubated for another 10 min. Chromatin was sonicated to an average length of 500 bp and clarified by centrifugation at 14,000 rpm for 15 min. Supernatants were pre-cleared with protein A agarose beads (Millipore) for 20 min and centrifuged at 500 *g* for 5 min. To immunoprecipitate protein/chromatin complexes, the supernatants were first diluted 10 times with IP dilution buffer (0.01% SDS, 1.1% Triton X 100, 1.2mM EDTA, 16.7mM Tris-Cl, pH 8.1, and 167mM NaCl), incubated with 1–3 μg of antibody overnight, followed by addition of 50 μL of protein A agarose bead for 2 h. After beads were washed four times with IP wash buffer (100mM Tris-Cl, pH 9.0, 500mM LiCl, 1% NP40, and 1% Deoxycholate), the antibody/protein/DNA complexes were eluted with 150 μL IP elution buffer (50mM NaHCO3, 1% SDS) for 15 min twice. To reverse the cross-links, 10 μg RNase A and 0.3M NaCl were added to the eluents at 65°C overnight. DNA/proteins were precipitated with ethanol, air-dried, and dissolved in 100 μL of TE. After proteins were digested by proteinase K at 45°C for 1 h, DNA was purified with DNA Clean & Concentrator-5 and eluted with 30 μL nuclease-free water. For initial ChIP-PCR validation, ChIPed-DNA will be diluted 1:10 in water and 5 μL diluted DNA will be used as a template for each qPCR reaction. ChIP-PCR primers targeting EZH2 targets will be designed using Primer3 software. The primer sequences were as follows: ZEB1:

5′-CGAGACCTGAACATGTGGTG-3′ (forward) and 5′-GCCCCGAGATAACCAGAAAT-3′ (reverse); ZEB2: 5′-GAGAAAGGAGATGGGGGTTC-3′ (forward) and 5′-CTCCAAAACGGACCTACCAA-3′ (reverse); Twist1: 5′-GGACTGGAAAGCGGAAACTT-3′ (forward) and 5′-ACGTGAGGAGGAGGGACTTT-3′ (reverse); SNAI1: 5′-CACTGGACCAGAAGCTACCC-3′ (forward) and 5′-GTGTGGGGCACTGTACCTG-3′

(reverse); SNAI2: 5′-CTTCCCCCTTCCTTTTTCAA-3′ (forward) and 5′-GCCTTGCACAAAGACCAAAT-3′ (reverse); CDH1: 5′-AGAAATTGCACTCCCACACC-3′ (forward) and 5′-GATCCCCAAATCTGCGTAAA-3′ (reverse).

2.10 | Dual-luciferase reporter assay

The ID of SNAIL and SLUG luciferase reporter plasmid are 31695 and 31694 (Addgene). After 48 h transfection, cells luciferase intensities were measured by Dual-Luciferase Reporter Assay System (#E1910; Promega). Firefly luciferase activity levels were normalized by Renilla luciferase activities.

2.11 | Statistical analysis

qPCR, ChIP-PCR, and the levels of EZH2 across different groups and databases were analyzed by an unpaired Student *t* test. The statistic of survival was calculated by the Kaplan–Meier log rank analysis. All data were presented as the mean ± standard deviation (SD) of each group. The analysis software was Graphpad Prism 8.0. The significant difference was uniformly set at $p < 0.05$.

3 | RESULTS

3.1 | EMT signature genes are highly expressed in human metastatic PCa

To investigate expression of EMT-relevant genes in human mCRPC, we explored differentially expressed genes (DEGs) in metastatic human PCa from published data sets. To minimize bias, we used overlapping analysis to figure out those genes highly expressed in both data sets (Taylor et al.[23] and Grasso et al.[24]). As shown in Figure 1A, a set of differentially expressed genes is significantly changed in human metastatic prostate tumor samples. Among those DEGs, the EMT signature genes are found to be upregulated in human metastatic prostate tumor samples in both data sets (red circle). To explore the function of those genes, we performed GO enrichment and KEGG pathway analyses. We annotated the DEGs by KEGG. The top results of each functional group are shown in Figure 1B,C. We then classified the EMT-associated pathways and observed that focal adhesion, regulation of actin skeleton, ECM-receptor interaction, were dysregulated. We next applied size-dependent enrichment analysis to map each gene cluster into pathways. Cluster maps of focal adhesion, and regulation of actin cytoskeleton pathways are shown in Figure 1D and S1. Inactivation of focal adhesion and regulation of actin cytoskeleton was observed in metastatic tumor samples in comparison to primary tumor samples. These data suggest that EMT-relevant genes are upregulated in mCRPC.

3.2 | A higher level of EZH2 is associated with poor prognosis in PCa

As shown in Figure 1A, a set of EMT signature genes were changed in human metastatic prostate tumor samples in both data sets. Of note, EZH2 is one of the top genes highly expressed in metastatic PCa samples, implying its important role in metastasis. To validate this observation, we explored data sets from TCGA and found that the level of EZH2 was also elevated in primary PCa comparing with normal prostate tissues (Figure 2A). We then evaluated the levels of EZH2 in human PCa tumors and found that the levels of EZH2 were

gradually elevated in tumors with higher grades. The *p*-value for EZH2 with respect to G6 tumors versus G7 tumors was 0.019, which is statistically significant. While the *p*-value for G7 tumors versus G8 tumors was 8.4e-5, the *p*-value for G8 tumors versus G9 tumors was 4e-11. The *p*-value for G9 versus G10 tumors was 0.17, indicating no significant difference, likely due to a small sample size of G10 group ($n = 4$) tumors. In general, the levels of EZH2 were clearly elevated in high-grade prostatic tumors (Figure 2B). Next, we investigated the levels of EZH2 in human PCa tumors with or without lymph node metastasis. As shown in Figure 2C, the levels of EZH2 were elevated in human PC tumors with lymph node metastasis (N1) comparing with nonlymph node metastasis (N0). To further study the levels of EZH2 in metastatic PCa tumors, we next explored several published data sets and found that, relative to primary PC tumors, the levels of EZH2 were significantly upregulated in metastatic PC tumors (Figure 2D). Not surprising, a higher level of EZH2 was associated with a shorter survival time, indicating the poor prognosis of human PCa patients (Figure 2E). The collective data suggest that the levels of EZH2 were elevated in metastatic PCa and associated with poor prognosis in human PCa patients.

3.3 | Enzalutamide-resistant PCa cells gain EMT features

In our previous study, we reported that chemotherapy-resistant CRPC expressing a higher level of β-catenin showed enrichment of cell adhesion and focal adhesion signature genes. These results implied that chemotherapy-resistant CRPC may possess EMT traits, as EMT is one of the mechanisms contributing to therapy resistance.[26] To test this concept, we dissected alterations of pathways in chemotherapy-sensitive and -resistant human PCa tumors. As illustrated in Figure 3A, the STAT3 pathway, NFκB pathway, focal adhesion, and ECM-receptor interaction pathway were activated in chemotherapy-resistant tumor samples, implying that metastasis might occur in these tumors.

Enzalutamide is a second-generation nonsteroidal antiandrogen clinically approved for the treatment of mCRPC. Unfortunately, most of the patients progresses to resistance to enzalutamide eventually, leading to the hypothesis that enzalutamide-resistant CRPC could gain more EMT properties. To explore the characteristics of enzalutamide-resistant cells, we performed IB by using antibodies against EMT markers in two pairs of isogenic PCa lines. As demonstrated in Figure 3B and S2, epithelial markers (E-cad and CK19) were decreased, whereas mesenchymal markers (N-cad and Vimentin) were increased in enzalutamide-resistant cells in comparison with their sensitive counterparts. Taken together, enzalutamide-resistant PCa cells gain more EMT features than that of enzalutamide-sensitive counterparts.

3.4 | Downregulation of EZH2 represses EMT

EMT is believed to play key role in tumor progression and metastasis by enabling a switch from the stationary epithelial-like cell phenotype to the motile mesenchymal phenotype. We also showed increased expression of EZH2 in advanced and metastatic prostate tumors (Figure 2A–D), suggesting that it may play a role in the process of EMT. The study of EZH2 in EMT aims to better understand the molecular mechanisms underlying prostate tumor progression and identify potential therapeutic targets for metastatic prostate cancer. To this end, we sought to investigate whether downregulation of EZH2 could attenuate EMT in PCa cells. To explore the role of EZH2 in metastasis, two classical

assays of cell motility were used. As demonstrated in Figure 4A,B, downregulation of EZH2 inhibited both wound closure and migration in EnzR cells. To further dissect how EZH2 contributes to EMT in EnzR cells, we depleted EZH2 with shRNA in C4-2R and MR49F cells, followed by IB. As shown in Figure 4C and S3A, downregulation of EZH2 resulted in reduction of mesenchymal-like markers (N-cadherin and Snail). Of note, the observations were independent of enzalutamide treatment. To determine whether such effects are PRC2 dependent, EnzR cells were treated with EPZ6438, a specific EZH2 inhibitor, followed by assessing EMT markers. Surprisingly, no significant changes of EMT markers were observed upon inhibition of EZH2 activity (Figure 4D). To probe the apparent PRC2 activity-independent function of EZH2, we depleted EZH2 and performed immunofluorescence (IF) staining against cell adhesion markers. Considering that weakening adherens junction (E-cadherin) and tight junction (JAM-A) enhance cell migration and EMT, we asked whether EZH2 disrupts cell junctions. As indicated, EZH2 downregulation enhanced the adherens junction (Figure 4E) and tight junction (Figure 4F and S3B). Collectively, EZH2 downregulation increases the expression of the epithelial-like markers, resulting in the enhancement of cell junction and prevention of cell migration. To further study the role of EZH2 in EMT, we then depleted EZH2 in $ARCaP_M$ cells, a specific mesenchymal PCa cell line, and followed by IF staining. In agreement, EZH2 downregulation restored the localization of E-cadherin at the areas of cell-cell contacts and the actomyosin cytoskeleton structure, indicating a profound assembly of adherens and tight junctions (Figure S3C). Taken together, these data suggest that EZH2 deletion inhibits a pro-motile phenotype by restoring intercellular adhesions.

3.5 | Downregulation of EZH2 inhibits expression of EMT-related transcription factors

On a molecular level, EMT is characterized by the decreased expression of epithelial markers and the increased expression of mesenchymal markers. To investigate whether downregulation of EZH2 antagonizes EMT in EnzR CRPC cell line, we examined several mesenchymal markers. As demonstrated, downregulation of EZH2 downregulated expression of mesenchymal markers (N-cadherin and fibronectin) (Figure 5A). In agreement, we found CDH1, an epithelial marker gene, was upregulated upon EZH2 deletion (Figure 5B).

Next, we sought to dissect the molecular mechanism(s) underlying potential EZH2-dependent regulation of EMT and metastasis. We sought to elucidate the signaling pathways downstream of EZH2 that are responsible for the EMT induction and increased motility of prostate epithelial cells. Epithelial cells undergoing EMT are characterized by expression of several regulators including SNAI1 (SNAIL), SNAI2 (SLUG), ZEB1, ZEB2, and TWIST.[27] Enzalutamide, a widely used form of androgen deprivation therapy, de-represses the EMT-promoting transcription factor Snail.[28] Therefore, we hypothesized that several transcriptional factors might be induced by EZH2 in prostate epithelial cells. To test this concept, we performed quantitative real-time PCR analysis and demonstrated that downregulation of EZH2 reduced transcriptions of ZEB1, ZEB2, TWIST, SNAIL, and SLUG, significantly (Figures 5C and 3D). In agreement, decreased protein levels of Twist and Snail were observed by IB upon EZH2 deletion (Figure 5D and S4). However, treatment with EZH2 inhibitors, GSK126 and EPZ6438, did not change the protein level of Snail,

indicating such regulation is PRC2 independent (Figure 5E). Next, we sought to determine whether EZH2 regulated the transcription of EMT transcription factor. As demonstrated in Figure 5F, We performed luciferase reporter assay and found depletion of EZH2 could decreases transcription of SNAIL and SLUG directly in C4-2R cells. These collective data suggest that deletion of EZH2 suppresses EMT via inhibiting the transcription of EMT-related transcription factors in a manner independent of PRC2.

3.6 | Deletion of EZH2 inhibits expression of EMT-associated transcription factors by impairing formation of H3K4me3 histone mark on the promotors

Next, we sought to investigate how EZH2 regulates expression of the transcription factors in ENZ-resistant PCa cells. The oncogenic function of EZH2 in cells of castration-resistant prostate cancer is independent of its role as a transcriptional repressor. Instead, it involves the ability of EZH2 to act as a coactivator for critical transcription factors, including androgen receptor.[20] In considering EZH2 being an epigenetic modulator that specifically catalyzes histone H3 lysine 27 trimethylation (H3K27me3), leading to epigenetic (defined as histone modifications) silencing of many tumor suppressor genes,[29] it renders the plausibility to hypothesize that EZH2 may regulate expression of EMT-related transcription factors by loading to targeted chromatins. To test, we explored the published database [29] and found that EZH2 could load to promoter regions of TWIST, SNAIL, SLUG, and ZEB1 genes, which can be attenuated by EZH2 downregulation (Figure 6A). Histone modifications, such as methylation, play important roles in regulation of gene expression. To dissect the underlying mechanisms contributing to the gene expressions, we performed chromatin immunoprecipitation assay, followed by real-time PCR to determine whether and how EZH2 deletion regulates gene expressions. As demonstrated in Figure 6B, downregulation of EZH2 impaired the formation of H3K4me3 but not H3K27Ac histone mark on the promoter regions of targeted transcription factors. Moreover, accompanying with the reduction of expressions of EMT-related transcription factors, elevation of an epithelial marker, CDH1 was observed upon EZH2 deletion. This finding further support the concept that EZH2 deletion could reverse EMT in EnzR PCa. Taken together, downregulation of EZH2 results in suppression of EMT-related transcription factors through impairing the formation of H3K4me3 histone mark on their promoter regions.

4 | DISCUSSION

Enzalutamide, being an oral AR inhibitor with a high affinity for its target, prevents AR nuclear translocation, DNA binding, and coactivator recruitment.[30] Despite the overall efficacy of enzalutamide in treating mCRPC,[2] individual patients have variable responses to treatment, and the eventual development of resistance is nearly universal. In addition, the administration of enzalutamide may also induce some unwanted adverse effects, including the development of enzalutamide resistance and metastasis.[31,32] Potential therapeutic targets for EnzR mCRPC have not been discovered yet. In the present study, we aim to ask whether and how EZH2 contributes to metastasis in EnzR CRPC. We demonstrated that EZH2 was highly expressed in mCRPC, implying an important role of EZH2 in EMT (Figures 1 and 2), and EnzR PCa cell lines harbor more EMT properties as expected (Figure 3).

Epithelial phenotypes are characterized by apical-basal cell polarity, intercellular adhesion and cohesive interaction, and lack of mobility of individual cells. Mesenchymal cells are completely different, being neither adherent nor apically polarized.[33] Accumulating evidence suggests that EMT promotes the occurrence and development of mCRPC, whilst some patients with mCRPC may even experience differentiation into highly aggressive neuroendocrine PCa.[34] In the present study, we observed that downregulation of EZH2 suppressed EnzR cell invasion and migration and reserved EMT. Downregulation of EZH2 also enhanced cell junctions of enzalutamide-resistant PCa cells (Figure 4).

EZH2 can function as a non-histone methyltransferase independent of the PRC2 complex[35,36] to methylate non-histone proteins, such as STAT3 and AR, thus promoting tumorigenicity.[6,20] However, the detailed mechanisms to switch histone to non-histone methyltransferase function of EZH2 are unclear. Interestingly, in CRPC cells, the oncogenic activity of EZH2 does not rely on the PRC2 complex, suggesting that this PRC2-independent function is also critical in CRPC cells. In this study, we observed the differences between EZH2 downregulation and inhibition by its pharmaceutical inhibitors. EZH2 downregulation could reverse EMT in EnzR PCa cells but not the EZH2 inhibitor, EPZ6438, indicating the role of EZH2 on EMT is PRC2 independent (Figure 4C,D).

Yuan et al.[21] have reported that AMPK-SETD2-EZH2 axis integrates metabolic and epigenetic signaling to restrict PCa metastasis. However, the mechanisms by which EZH2 contributing to enzalutamide-resistant metastasis remains unclear. Epithelial cells undergoing EMT are characterized by the expression of several regulators, including SNAI1 (SNAIL), SNAI2 (SLUG), ZEB1, ZEB2, and TWIST.[27] Herein, we measured the transcription of these transcription factors and found EZH2 downregulation induced downregulation of these TFs (Figure 5). Xu et al.[20] have reported that only EZH2 binding peaks are enriched for the active histone marks H3K4 dimethylation and trimethylation (H3K4me2 and H3K4me3), suggesting the potential functions of these peaks in gene activation. By exploring the published database, we found that EZH2 could bind to the promotor regions of these TFs, indicating the epigenetic roles of EZH2 in modulating gene activation (Figure 6A). Furthermore, we performed ChIP-PCR to investigate the formation of the H3K4me3 histone mark on the promotor regions of these genes. As demonstrated, H3K4me3 but not H3K27Ac histone mark did form on the promotor regions of these genes (Figure 6B).

In summary, EZH2 was highly expressed in EnzR CRPC, and downregulation of EZH2 could attenuate EMT in EnzR CRPC cells. EZH2 facilitates the formation of H3K4me3 histone marks on the promotor regions of transcription factors in these cells. Even though our findings imply the potential of EZH2 to be a target for treating mCRPC, particularly in those patients showing limited response to enzalutamide, additional studies are warranted to clarify the potential to treat mCRPC within various mouse tumor models. Because the suppressive effects of EZH2 on EMT are PRC2-independent and most of EZH2 inhibitor targeting its catalytic activity, the novel pharmaceutical inhibitors targeting PRC2-independent activities are needed for further study.

Supplementary Material

Refer to Web version on PubMed Central for supplementary material.

ACKNOWLEDGMENTS

This research was supported by NIH R01 CA157429 (X. Liu), NIH R01 CA264652 (X. Liu), NIH R01 CA256893 (X. Liu), and NIH R01 CA196634 (X. Liu). This research was also supported by the Biospecimen Procurement & Translational Pathology, Biostatistics and Bioinformatics, Flow Cytometry, and Immune Monitoring Shared Resources of the University of Kentucky Markey Cancer Center (P30CA177558).

DATA AVAILABILITY STATEMENT

The data that support the findings of this study are openly available in Gene Expression Omnibus (GEO, https://www.ncbi.nlm.nih.gov/geo).

REFERENCES

1. Ryan CJ, Smith MR, de Bono JS, et al. Abiraterone in metastatic prostate cancer without previous chemotherapy. N Engl J Med. 368, 2013:138–148. [PubMed: 23228172]
2. Beer TM, Armstrong AJ, Rathkopf DE, et al. Enzalutamide in metastatic prostate cancer before chemotherapy. N Engl J Med. 2014;371:424–433. [PubMed: 24881730]
3. Varambally S, Dhanasekaran SM, Zhou M, et al. The polycomb group protein EZH2 is involved in progression of prostate cancer. Nature. 2002;419:624–629. [PubMed: 12374981]
4. Sanulli S, Justin N, Teissandier A, et al. Jarid2 methylation via the PRC2 complex regulates H3K27me3 deposition during cell differentiation. Mol Cell. 2015;57:769–783. [PubMed: 25620564]
5. Ardehali MB, Anselmo A, Cochrane JC, Kundu S, Sadreyev RI, Kingston RE. Polycomb repressive complex 2 methylates elongin A to regulate transcription. Mol Cell. 2017;68, 872–884. [PubMed: 29153392]
6. Kim E, Kim M, Woo DH, et al. Phosphorylation of EZH2 activates STAT3 signaling via STAT3 methylation and promotes tumorigenicity of glioblastoma stem-like cells. Cancer Cell. 2013;23:839–852. [PubMed: 23684459]
7. Takaya T, Kawamura T, Morimoto T, et al. Identification of p300-targeted acetylated residues in GATA4 during hypertrophic responses in cardiac myocytes. J Biol Chem. 2008;283:9828–9835. [PubMed: 18252717]
8. Lee JM, Lee JS, Kim H, et al. EZH2 generates a methyl degron that is recognized by the DCAF1/DDB1/CUL4 E3 ubiquitin ligase complex. Mol Cell. 2012;48:572–586. [PubMed: 23063525]
9. Park SH, Fong K, Kim J, et al. Posttranslational regulation of FOXA1 by polycomb and BUB3/USP7 deubiquitin complex in prostate cancer. Sci Adv. 2021;7(15):eabe2261. [PubMed: 33827814]
10. Lu H, Li G, Zhou C, et al. Regulation and role of post-translational modifications of enhancer of zeste homologue 2 in cancer development. Am J Cancer Res. 2016;6:2737–2754. [PubMed: 28042497]
11. Cha TL, Zhou BP, Xia W, et al. Akt-mediated phosphorylation of EZH2 suppresses methylation of lysine 27 in histone H3. Science. 2005;310:306–310. [PubMed: 16224021]
12. Palacios D, Mozzetta C, Consalvi S, et al. TNF/p38α/polycomb signaling to Pax7 locus in satellite cells links inflammation to the epigenetic control of muscle regeneration. Cell Stem Cell. 2010;7:455–469. [PubMed: 20887952]
13. Lee CH, Yu JR, Granat J, et al. Automethylation of PRC2 promotes H3K27 methylation and is impaired in H3K27M pediatric glioma. Genes Dev. 2019;33:1428–1440. [PubMed: 31488577]
14. Tang X, Milyavsky M, Shats I, Erez N, Goldfinger N, Rotter V. Activated p53 suppresses the histone methyltransferase EZH2 gene. Oncogene. 2004;23:5759–5769. [PubMed: 15208672]

15. Bracken AP, Kleine-Kohlbrecher D, Dietrich N, et al. The polycomb group proteins bind throughout the INK4A-ARF locus and are disassociated in senescent cells. Genes Dev. 2007;21:525–530. [PubMed: 17344414]
16. Bryant RJ, Cross NA, Eaton CL, Hamdy FC, Cunliffe VT. EZH2 promotes proliferation and invasiveness of prostate cancer cells. Prostate. 2007;67:547–556. [PubMed: 17252556]
17. Yu J, Cao Q, Mehra R, et al. Integrative genomics analysis reveals silencing of β-adrenergic signaling by polycomb in prostate cancer. Cancer Cell. 2007;12:419–431. [PubMed: 17996646]
18. Min J, Zaslavsky A, Fedele G, et al. An oncogene–tumor suppressor cascade drives metastatic prostate cancer by coordinately activating Ras and nuclear factor-κB. Nature Med. 2010;16:286–294. [PubMed: 20154697]
19. Yang YA, Yu J. EZH2, an epigenetic driver of prostate cancer. Protein Cell. 2013;4:331–341. [PubMed: 23636686]
20. Xu K, Wu ZJ, Groner AC, et al. EZH2 oncogenic activity in castration-resistant prostate cancer cells is polycomb-independent. Science. 2012;338:1465–1469. [PubMed: 23239736]
21. Yuan H, Han Y, Wang X, et al. SETD2 restricts prostate cancer metastasis by integrating EZH2 and AMPK signaling pathways. Cancer Cell. 2020;38:350–365. [PubMed: 32619406]
22. Bai Y, Zhang Z, Cheng L, et al. Inhibition of enhancer of zeste homolog 2 (EZH2) overcomes enzalutamide resistance in castration-resistant prostate cancer. J Biol Chem. 2019;294:9911–9923. [PubMed: 31085587]
23. Taylor BS, Schultz N, Hieronymus H, et al. Integrative genomic profiling of human prostate cancer. Cancer Cell. 2010;18:11–22. [PubMed: 20579941]
24. Grasso CS, Wu YM, Robinson DR, et al. The mutational landscape of lethal castration-resistant prostate cancer. Nature. 2012;487:239–243. [PubMed: 22722839]
25. Chandrashekar DS, Bashel B, Balasubramanya SAH, et al. UALCAN: a portal for facilitating tumor subgroup gene expression and survival analyses. Neoplasia. 2017;19:649–658. [PubMed: 28732212]
26. Zhang Z, Cheng L, Li J, et al. Inhibition of the Wnt/β-catenin pathway overcomes resistance to enzalutamide in castration-resistant prostate cancer. Cancer Res. 2018;78:3147–3162. [PubMed: 29700003]
27. Sánchez-Tilló E, Liu Y, de Barrios O, et al. EMT-activating transcription factors in cancer: beyond EMT and tumor invasiveness. Cell Mol Life Sci. 2012;69:3429–3456. [PubMed: 22945800]
28. Sidaway P. Enzalutamide promotes mesenchymal plasticity via Snail activation. Nat Rev Urol. 2017;14:325.
29. Kim J, Lee Y, Lu X, et al. Polycomb- and methylation-independent roles of EZH2 as a transcription activator. Cell Rep. 2018;25:2808–2820. [PubMed: 30517868]
30. Buttigliero C, Tucci M, Bertaglia V, et al. Understanding and overcoming the mechanisms of primary and acquired resistance to abiraterone and enzalutamide in castration resistant prostate cancer. Cancer Treat Rev. 2015;41:884–892. [PubMed: 26342718]
31. Lin TH, Izumi K, Lee SO, Lin WJ, Yeh S, Chang C. Anti-androgen receptor ASC-J9 versus anti-androgens MDV3100 (Enzalutamide) or Casodex (Bicalutamide) leads to opposite effects on prostate cancer metastasis via differential modulation of macrophage infiltration and STAT3-CCL2 signaling. Cell Death Dis. 2013;4:e764. [PubMed: 23928703]
32. Qin J, Lee HJ, Wu SP, et al. Androgen deprivation-induced NCoA2 promotes metastatic and castration-resistant prostate cancer. J Clin Invest. 2014;124:5013–5026. [PubMed: 25295534]
33. Larue L, Bellacosa A. Epithelial-mesenchymal transition in development and cancer: role of phosphatidylinositol 3' kinase/AKT pathways. Oncogene. 2005;24:7443–7454. [PubMed: 16288291]
34. Li P, Yang R, Gao WQ. Contributions of epithelial-mesenchymal transition and cancer stem cells to the development of castration resistance of prostate cancer. Mol Cancer. 2014;13:55. [PubMed: 24618337]
35. Hock H. A complex polycomb issue: the two faces of EZH2 in cancer. Genes Dev. 2012;26:751–755. [PubMed: 22508723]
36. Kim KH, Roberts CWM. Targeting EZH2 in cancer. Nature Med. 2016;22:128–134. [PubMed: 26845405]

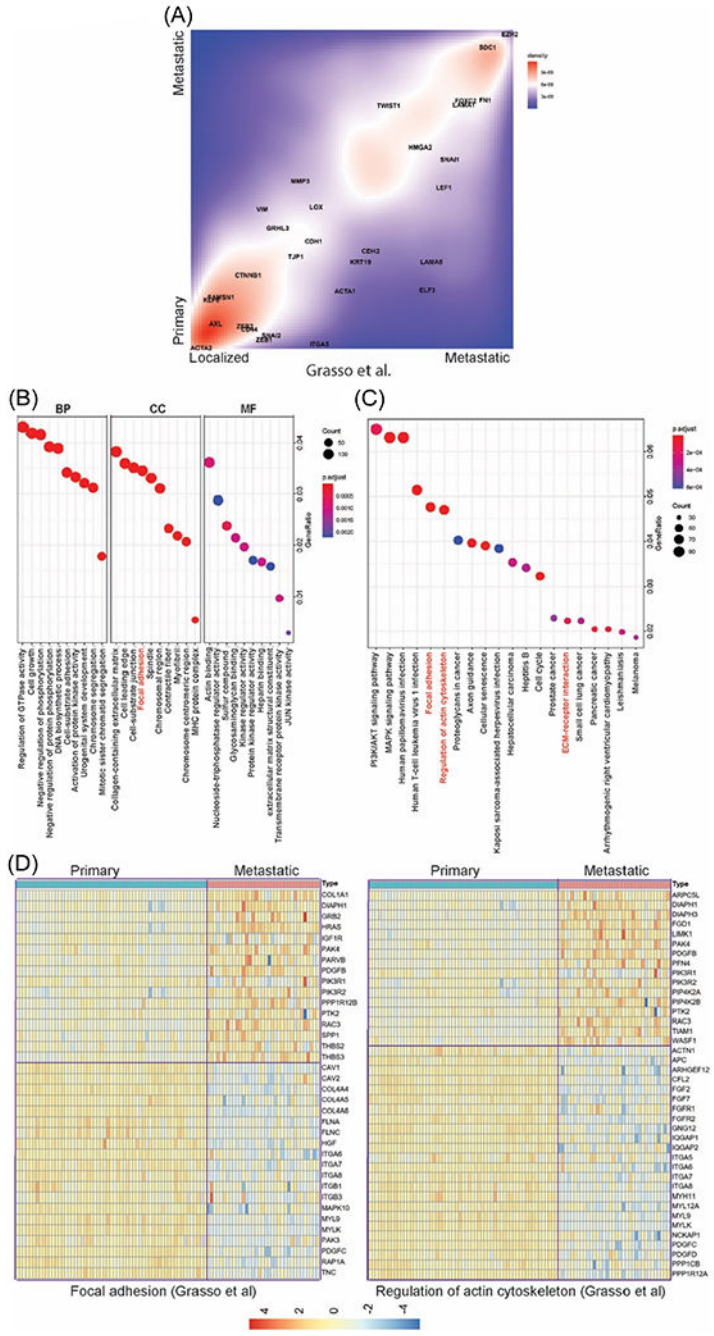

FIGURE 1.

Identifying EMT signature genes and pathways in metastatic PCa. (A) 2-D density plot to illustrate the overlapping DEGs in localized and metastatic prostate tumor specimens from two human PCa data sets. The high heat area along the diagonal indicates significant overlap in DEGs between the two data sets. The color bar indicates *p*-value between two ordered gene sets. Selected epithelial and EMT signature genes were plotted corresponding to their signed and logged *p*-value ranks based on differential expression between metastatic and primary cancer samples. A number of EMT signature genes (large red circle) were

consistently ranked at similar positions in both human PCa data sets. EZH2 (small green circle) was among the group of genes differentially expressed in metastatic PCa in both human data sets. (B) Significantly enriched gene ontology (GO) items for differentially transcribed genes between the localized and metastatic prostate tumor specimens. (C) Top KEGG pathway enrichment scatter plot of DEGs. (D) Heatmaps showing DEGs in each pathway comparing between primary and metastatic prostate tumor specimens from the Grasso et al.[24] data set. BP, biological process; CC, cellular component; DEGs, differentially expressed genes; EMT, epithelial–mesenchymal transition; KEGG, Kyoto Encyclopedia of Genes and Genomes; MF, molecular function; PCa, prostate cancer.

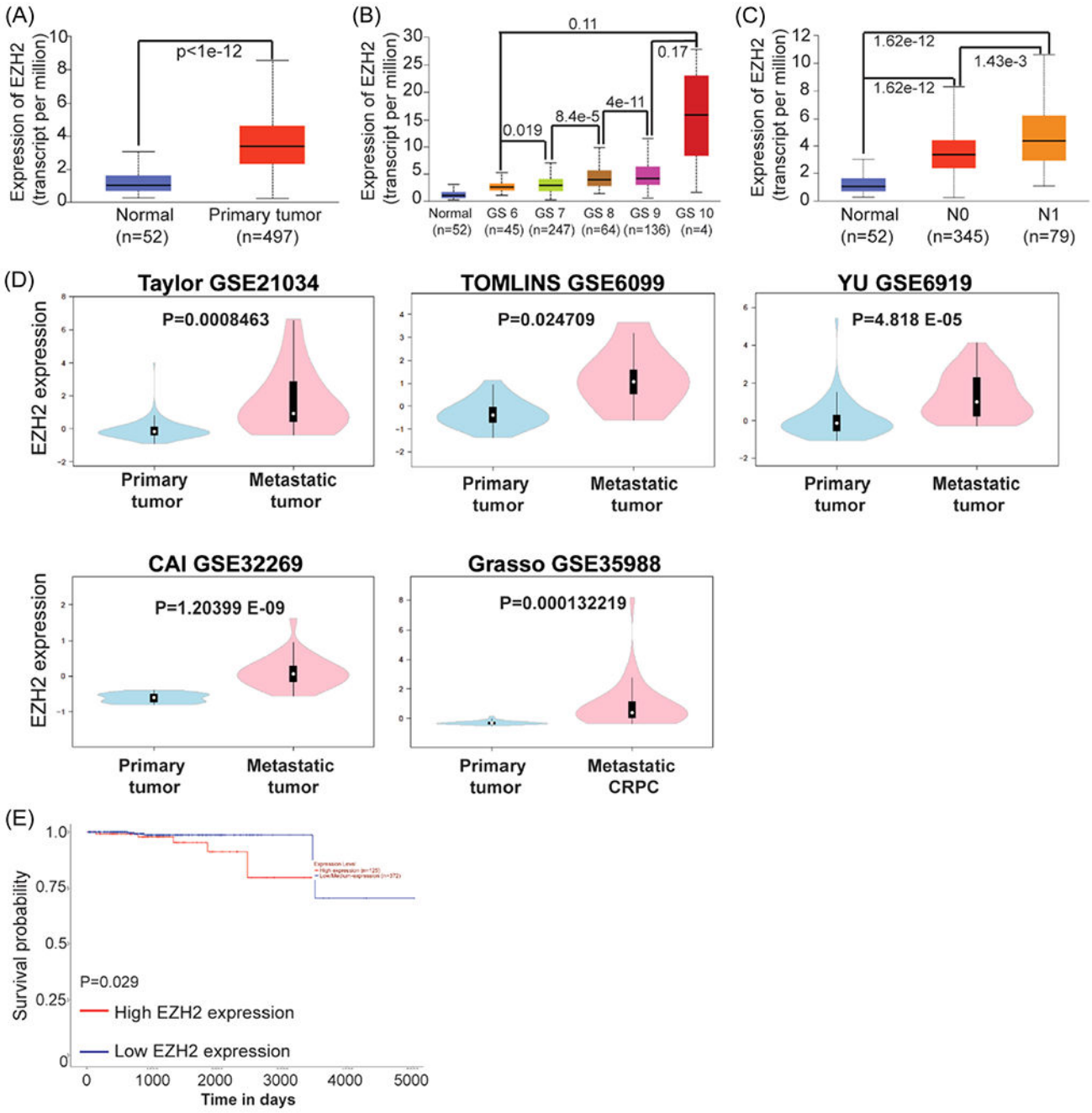

FIGURE 2.

EZH2 is highly expressed in mCRPC. (A) Comparison of the transcriptional levels of EZH2 between normal tissues and primary PCa tumors from TCGA database. (B) The levels of EZH2 in PCa patient tumors with different Gleason scores (GS). (C) The levels of EZH2 in patient tumors with or without lymph node metastasis. (D) Data shown (y-axis) are Z-scores of microarray expression values for GSE6919, GSE35988, GSE6099, GSE32269, and GSE21034P values between primary and metastatic PCa were calculated using unpaired two-sided *t*-tests. Violin plots represent the median and the first and third quartiles; Whisker

edges indicate the minimum and maximum value. (E) Survival analysis of PCa patients from TCGA database with different levels of EZH2. All the data in (A), (B), (C), and (E) were performed with a published online tool.[25] mCRPC, metastatic castration-resistant prostate cancer; PCa, prostate cancer; TCGA, The Cancer Genome Atlas.

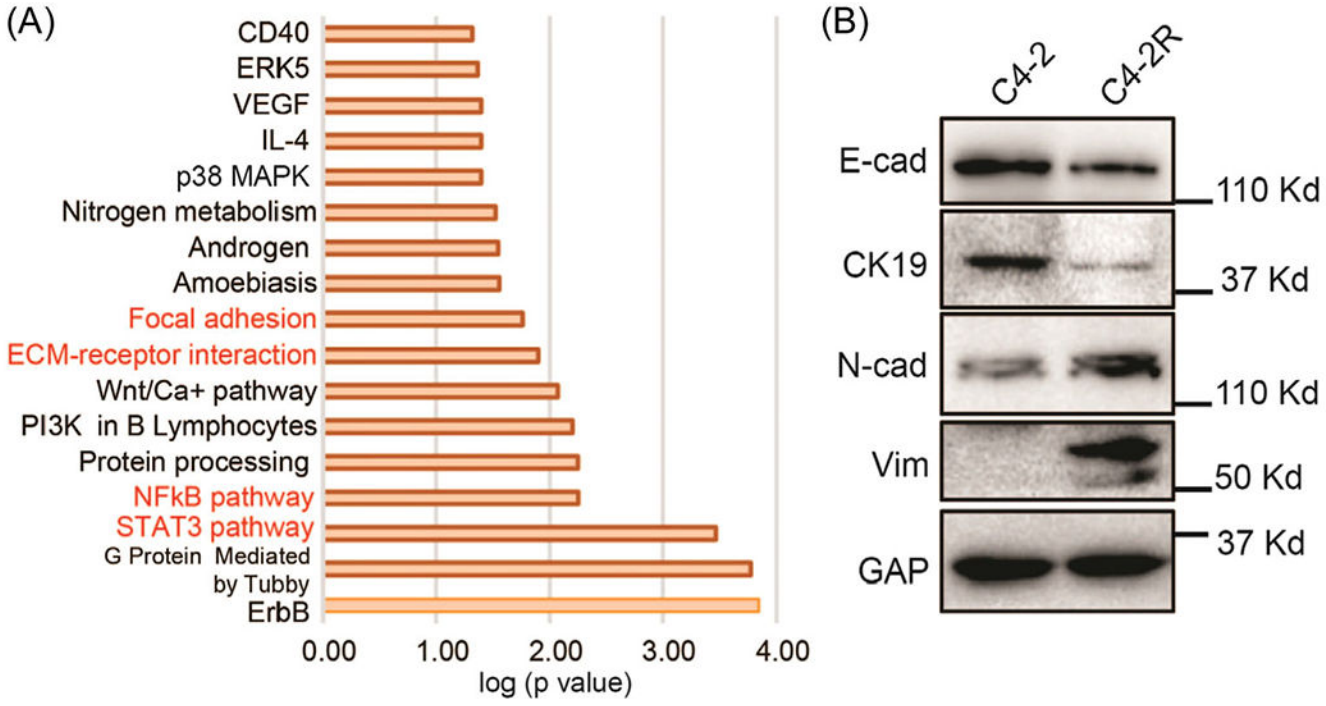

FIGURE 3.

Enzalutamide-resistant PCa cells gain more EMT properties. (A) GO pathway analysis in chemotherapy-sensitive versus -resistant PCa specimens. (B) Cell lysates were prepared from the indicated PCa cell lines and subjected to immunoblotting (IB). EMT, epithelial–mesenchymal transition; GO, Gene Ontology; PCa, prostate cancer.

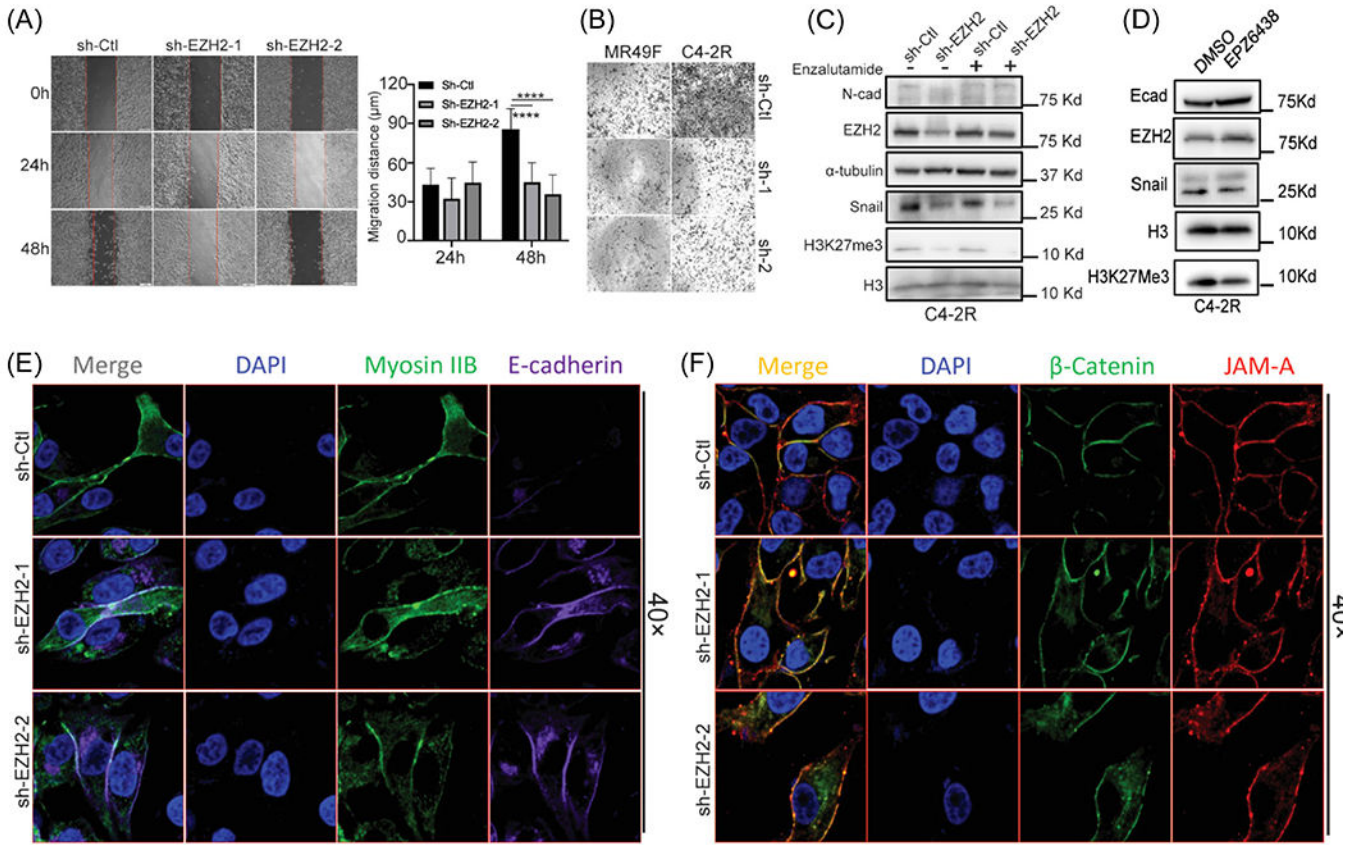

FIGURE 4.

Downregulation of EZH2 suppresses EMT. (A) C4-2R cells with downregulation of EZH2 were subjected to a wound healing assay. (B) C4-2R and MR49F were depleted with EZH2, and subjected to in vitro 48 h migration assay. (C) Cell lysates from C4-2R cells with downregulation of EZH2 and with or without enzalutamide treatment (20uM) were prepared and subjected to IB. (D) C4-2R cells were treated with EPZ6438 (25 μM) for 24 h, followed by IB to detect EMT markers. (E) and (F) C4-2R cells with downregulation of EZH2 were subjected to IF staining to assess adhesion junction (E-cadherin and β-catenin labeling) and tight junction (JAM-A) and the actomyosin cytoskeleton (myosin IIB) (Magnification: 40×). EMT, epithelial–mesenchymal transition.

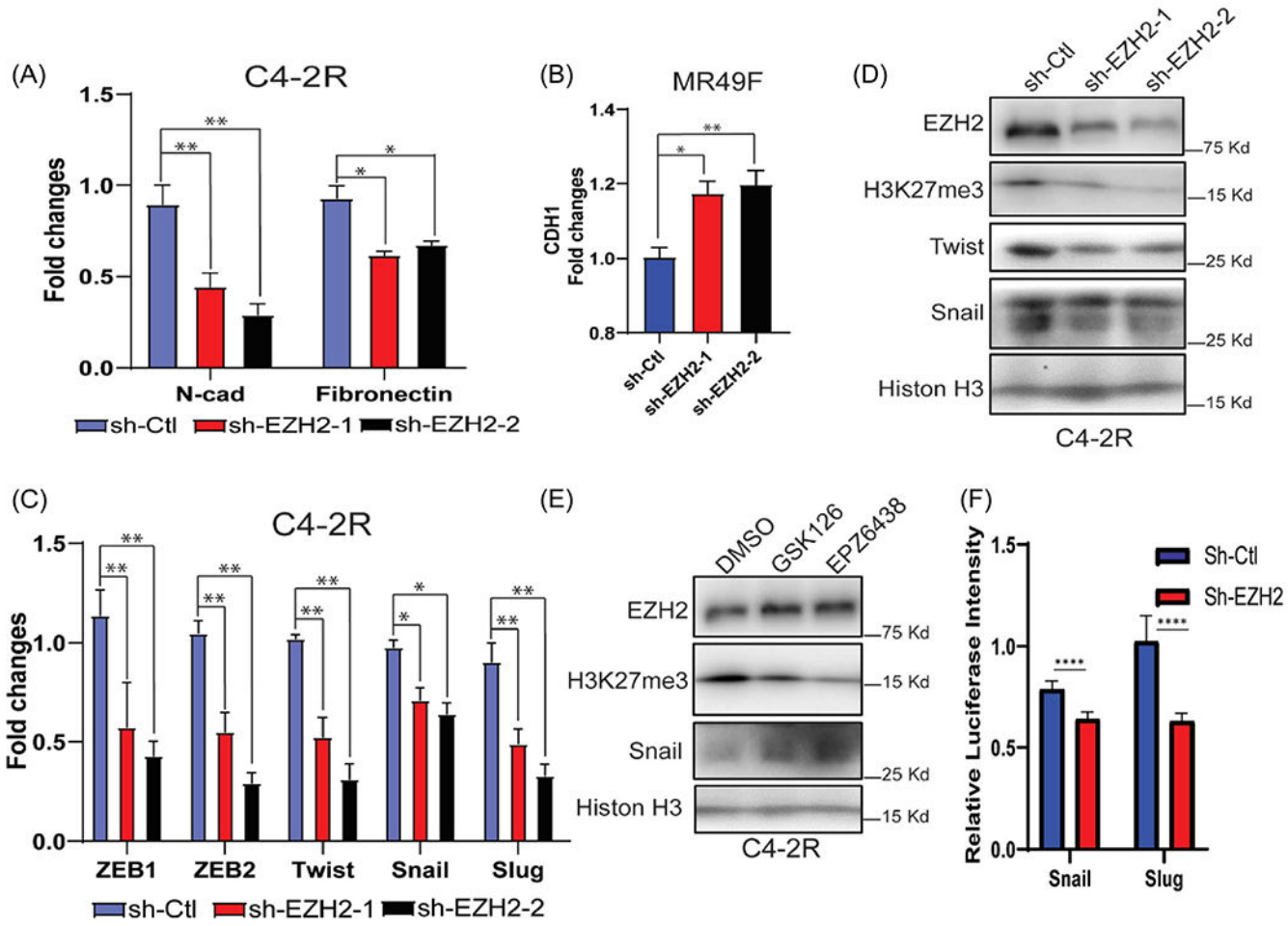

FIGURE 5.

Downregulation of EZH2 inhibits expression of EMT-associated transcription factors. (A) C4-2R cells were depleted with EZH2, followed by qPCR to measure expression of mesenchymal markers. (B) MR49F cells were depleted with EZH2, followed by qPCR to measure expression of CDH1. (C) C4-2R cells were depleted with EZH2, followed by qPCR to measure expression of EMT-associated transcription factors. (D) Cell lysates from C4-2R cells with downregulation of EZH2 were prepared and subjected to IB. (E) Cell lysates from C4-2R cells treated with EZH2 inhibitors were subjected to IB. *$p < 0.05$, **$p < 0.01$. (F) C4-2R cells were transfected with SNAIL and SLUG luciferase reporter. The luciferase activity was determined as above. EMT, epithelial–mesenchymal transition; qPCR, quantitative polymerase chain reaction.

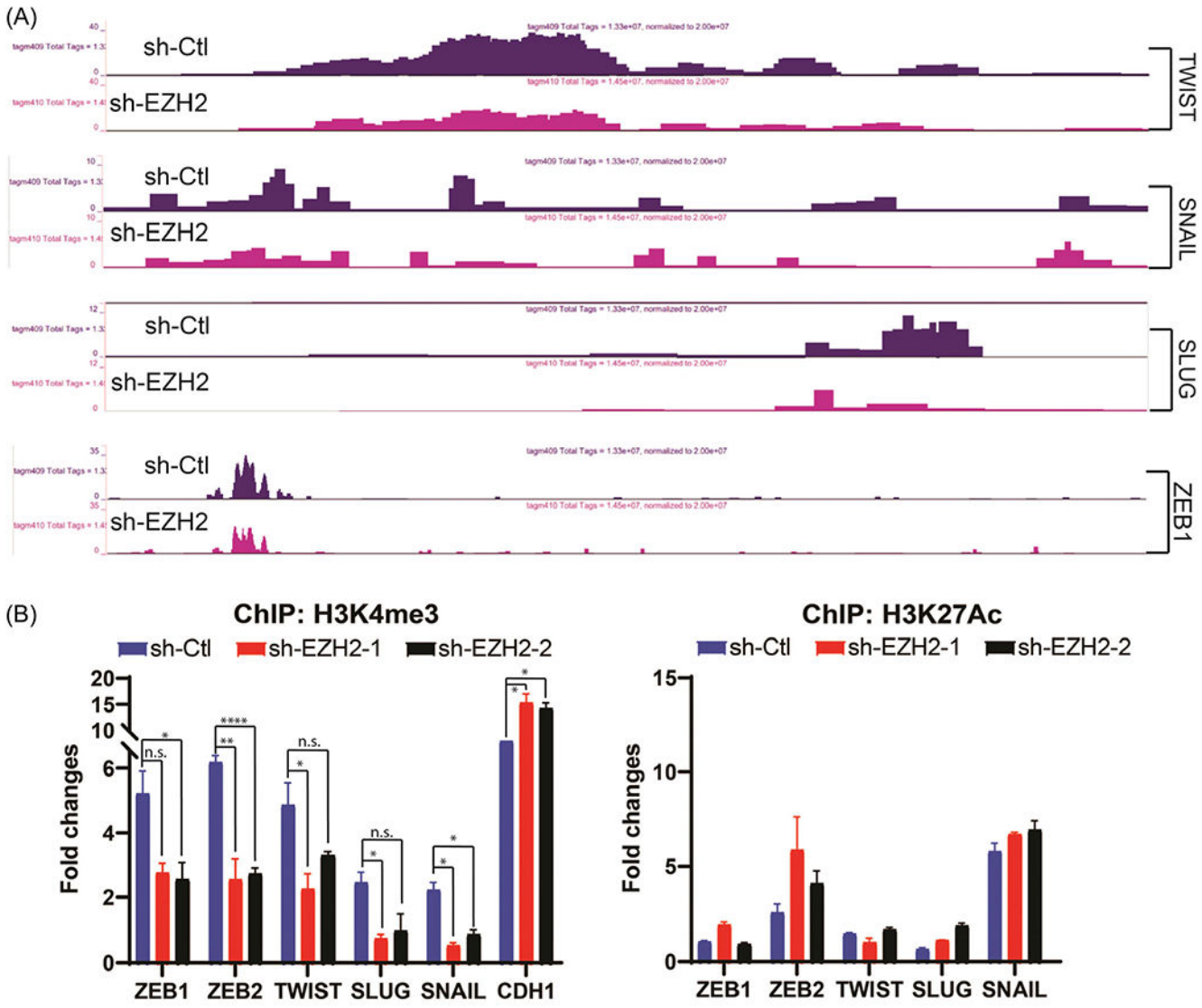

FIGURE 6.

Downregulation of EZH2 impairs loading of H3K4me3 to the promotor regions. (A) ChIP-seq analysis within the published data (GSE107782). (B) ChIP with anti-H3K4me3 (left) and anti-H3K27Ac (right) and followed by qPCR to measure the binding abilities to the indicated genes' promotor regions. *$p < 0.05$, **$p < 0.01$, ****$p < 0.0001$. ChIP, chromatin immunoprecipitation; ns, not significant; qPCR, quantitative polymerase chain reaction.